INTERNATIONAL JOURNAL FOR NUMERICAL METHODS IN FLUIDS, VOL. 19, 997–1012 (1994)

EFFICIENT HIGHER-ORDER BACKWARD CHARACTERISTICS SCHEMES FOR TRANSIENT ADVECTION

T. S. YU AND C. W. LI

Department of Civil and Structural Engineering, Hong Kong Polytechnic, Hong Kong

SUMMARY

The use of the highest-order ($(N-1)$th-order) Lagrangian interpolation polynomial for the approximation of the exact solution in the backward characteristics scheme with N nodes is inefficient owing to the excessive number of terms in the polynomial. New schemes based on a combination of lower-order polynomials to approximate the exact solution are developed, with the relative weighting of the polynomials determined by Fourier mode analysis. With the addition of a flux limiter and a modified discriminator, the resulting schemes are oscillation-free, highly accurate, efficient and more cost-effective as compared with those schemes using the highest-order Lagrangian polynomial.

KEY WORDS Advection Method of characteristics Finite difference, Flux limiter

INTRODUCTION

A tremendous number of explicit finite difference schemes have been developed for the solution of the unsteady advection equation during the past several decades. Typical schemes are summarized as follows. The first-order upwind scheme[1] is the simplest scheme but introduces large numerical diffusion to the solution. The second-order leapfrog[2] and Lax–Wendroff[3] schemes eliminate numerical diffusion but introduce significant phase error to the solution. Fromm's second-order method of zero average phase error[4] seems to be the best second-order scheme. The third-order QUICKEST[5] scheme eliminates both the diffusive and phase errors arising from the first- and second-derivative terms and is widely used.

In parallel, the backward characteristics method with Lagrangian interpolative approximation of the exact solution has been used in the solution of the same equation.[6–8] Under constant velocity the scheme using two-node linear interpolation is equivalent to the first-order upwind finite difference scheme, the scheme using three-node quadratic interpolation[6] is equivalent to the Lax–Wendroff scheme and the scheme using four-node cubic interpolation is equivalent to the QUICKEST scheme.[8] Also, the scheme using quadratic interpolation over four nodes[9] is equivalent to Fromm's second-order method of zero average phase error. In situations where the solution profile is sharp but smooth, the use of the above low-order (up to third-order) Lagrangian interpolation scheme may not be accurate enough and a higher-order scheme is required.

Instead of using a Lagrangian polynomial, a Hermitian polynomial, which utilizes the unknown scalar and its spatial derivatives as dependent variables in the interpolation, has also

CCC 0271-2091/94/230997-16

Received January 1994
Revised June 1994

been employed. The scheme with two-node Hermitian cubic interpolation (2PHC)[10] is found to be quite accurate but requires the solution of four equations (one for the scalar and the rest for the scalar's spatial derivatives) in two dimensions, which leads to a complicated algorithm for dispersion or hydrodynamics modelling. To retain the accuracy of 2PHC and avoid using scalar derivatives as dependent variables, the six-node[11] quasi-Hermite interpolation scheme was developed.

Another natural extension of the backward characteristics method to higher order is to use an N-node scheme with an $(N-1)$th-order Lagrangian interpolative polynomial (the highest-order Lagrangian polynomial). The ULTIMATE schemes[8] were developed along this line. However, the number of terms involved in such schemes can be excessive, e.g. a six-node fifth-order (6P5I) scheme has 31 terms in the finite difference expression while an eight-node seventh-order (8P7I) scheme has 57 terms in the finite difference expression. Also, the accuracy produced by this type of interpolation may not be the highest as compared with other schemes requiring the same number of nodes.

This paper presents the development of a subclass of the backward characteristics scheme in which the interpolative approximation of the exact solution is based on a combination of several lower-order Lagrangian polynomials for a given number of nodes used in the computation. Fourier mode analysis is used to determine the optimal weighting of the various polynomials employed in the scheme. A flux limiter is employed to suppress numerical oscillation and a modified discriminator is developed to preserve the physical peak. Typical test examples are used to illustrate the accuracy and efficiency of the scheme.

GOVERNING EQUATION AND FOURIER MODE ANALYSIS

The one-dimensional pure advection of scalar C with constant positive velocity U is considered:

$$\frac{\partial C}{\partial t} + U\frac{\partial C}{\partial x} = 0, \tag{1}$$

where t is the time and x is the spatial co-ordinate. In Fourier mode anlaysis the initial condition of (1) is assumed to be a Fourier mode, $C_0 \exp[\sqrt{(-1)}\sigma x]$, where C_0 is the amplitude, $\sigma = 2\pi/L$ is the spatial frequency and L is the wavelength. The solution to the equation is given by

$$C(x, t) = C_0 \exp[\sqrt{(-1)}\sigma(x - Ut)]. \tag{2}$$

The propagation of the solution from time $n\Delta t$ to $(n+1)\Delta t$ is

$$C^{n+1} = C^n \exp[-\sqrt{(-1)}\sigma U\Delta t] = \lambda C^n, \tag{3}$$

where Δt is the time step and λ is called the propagation factor. The corresponding propagation factor λ' of a particular scheme can be obtained by substituting the Fourier mode expression into the finite difference expression of the scheme. The accuracy of the scheme can be assessed by comparing its propagation factor with that of the analytical solution. For an ideal numerical scheme both the amplitude ratio $|\lambda'|/|\lambda|$ and the celerity ratio $\arg(\lambda')/\arg(\lambda)$ should be equal to unity.

DEVELOPMENT OF THE NUMERICAL SCHEMES

Equation (1) states that the scalar C is invariant along a characteristic line. To determine the unknown scalar at node i and time level $n+1$, C_i^{n+1}, the characteristics line

$$\frac{dx}{dt} = U \tag{4}$$

passing through node i at time level $n+1$ is traced backwards in time to level n and the invariant scalar value is obtained at known time level n by means of polynomial interpolation:

$$C_i^{n+1} = C(i\Delta x, (n+1)\Delta t) = C(i\Delta x - U\Delta t, n\Delta t) = C^*, \tag{5}$$

where Δx is the space step. The interpolation polynomial chosen should pass through the nodal value C_i^n and preferably pass through the nodal value C_{i-1}^n, because the resulting finite difference expression will then give the exact solution when the Courant number v ($=U\Delta t/\Delta x$) is zero or one.

If more than two nodes are involved in the computation, a Lagrangian polynomial can always be constructed to pass through all the nodal values. If three points are involved, there are two such quadratic polynomials, one passing through nodal values C_{i-1}^n, C_i^n, and C_{i+1}^n and the other passing through C_{i-2}^n, C_{i-1}^n and C_i^n. The former is found to have a better accuracy and is equivalent to the Lax–Wendroff scheme. If four points are involved, the cubic polynomial that produces a stable and accurate solution is that passing through nodal values C_{i-2}^n, C_{i-1}^n, C_i^n and C_{i+1}^n. The resulting scheme is found to be equivalent to the widely used QUICKEST scheme.

For a higher-order scheme in which $2r$ nodes are involved, the general expression can be written as

$$C_i^{n+1} = \sum_{k=-r}^{r-1} \frac{(v-r)*\cdots*(v-k+1)*(v-k-1)*\cdots*(v+r-1)}{(k-r)*\cdots*1*(-1)*\cdots*(k+r-1)} C_{i+k}^n = \sum_{k=-r}^{r-1} f_{i+k}(v) C_{i+k}^n. \tag{6}$$

Only schemes with an even number of nodes are considered, because numerical experiments indicate that schemes with an odd number of nodes have relatively large phase error. There are four desirable properties that the schemes possess.

1. $C_i^{n+1} = C_i^n$ when $v = 0$.
2. $C_i^{n+1} = C_{i-1}^n$ when $v = 1$.
3. Consistency requirement. If $C_i^n = C_0$ $\forall i$, then $C_i^{n+1} = C_0$ for any value of v.
4. Symmetry property. For transient advection in the positive direction with Courant number v, the value of C_i^{n+1} is given by equation (6). For transient advection in the negative direction with Courant number μ ($=V\Delta t/\Delta x$), the value of C_j^{n+1} is given by

$$C_j^{n+1} = \sum_{k=-r}^{r-1} f_{j+k}(\mu) C_{j+k}^n. \tag{7}$$

Comparing Figures 1(a) and 1(b), if $\mu = 1 - v$ and the nodal numbering system is such that $j + k = i - k - 1$, then we have

$$C_j^{n+1} = C_i^{n+1} \quad \Rightarrow \quad f_{i+k}(v) = f_{i-k-1}(1-v) \quad \forall k. \tag{8}$$

However, for higher-order schemes the criterion that the interpolative polynomial should pass

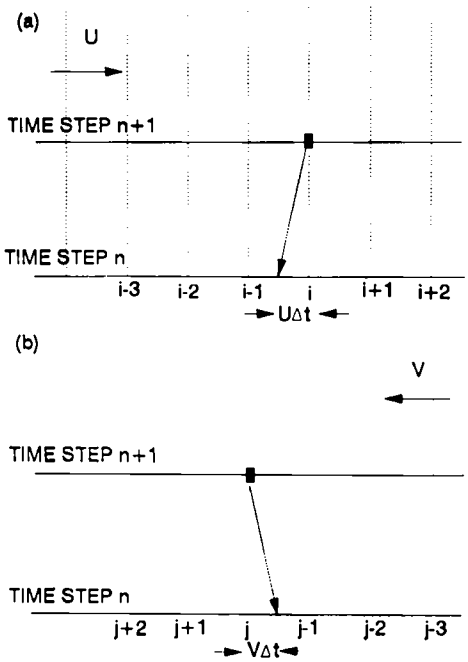

Figure 1. Illustration of the symmetry property of the backward characteristics method

all the nodal values may not be necessary and the approximation produced by such a polynomial may not be the most accurate. Also, an excessive number of terms are involved in the polynomial, which reduces the computational efficiency.

To save computational effort and to attempt to improve the accuracy, a class of schemes using lower-order interpolation polynomials is developed based on the following criteria. For a $2r$-node scheme the scheme is formed by a combination of rth-order polynomials which all pass through nodal values C_i^n and C_{i-1}^n (these polynomials process properties 1–3 above) Property 4 is satisfied by choosing the following pair of polynomials: one passes through nodal values $C_{i-I}^n, \ldots, C_{i-1}^n$, $C_i^n, \ldots, C_{i+J}^n$, and the other passes through $C_{i-J-1}^n, \ldots, C_{i-1}^n, C_i^n, \ldots, C_{i+I-1}^n$, where I and J are natural numbers. The optimal weighting of each polynomial is determined by means of Fourier mode analysis. The criteria for the selection of the scheme are that the integrated absolute error of the amplitude ratio over the whole spectrum is minimum and both the amplitude ratio and phase accuracy of the selected scheme are at least equal to those of the scheme using $(2r-1)$th-order polynomials. It has been found subsequently that the optimal weighting of each polynomial is dependent approximately linearly on v and hence the weighting coefficient is expressed as a linear function of v. Assume the expression of the scheme can be written as

$$C_i^{n+1} = \sum_k \alpha_k(v) L_k, \tag{9}$$

where the α_k are the weighting parameters (linear function of v) of the polynomials L_k. The consistency requirements give $\sum \alpha_k = 1$ and the symmetry property gives $\alpha_{i-k}(v) = \alpha_{1+k-1}(1-v)$.

For the four-node scheme (4P3O) there are two second-order polynomials which pass through consecutive nodal values including C_i^n and C_{i-1}^n. One is S_1 which passes through C_{i-1}^n, C_i^n and

C_{i+1}^n and the other is S_2 which passes through C_{i-2}^n, C_{i-1}^n and C_i^n. The expressions for S_1 and S_2 are given in Appendix I. The resulting scheme which satisfies properties 1–4 is given by

$$C_i^{n+1} = [a + (1 - 2a)v] * S_1 + [(1 - a) + (2a - 1)v] * S_2, \tag{10}$$

where a is a free parameter determined as $\frac{2}{3}$ from Fourier mode analysis. The full expression of 4P3O is given by

$$\begin{aligned} C_i^{n+1} = \tfrac{1}{6}[&(-v^3 + 3v^2 - 2v)C_{i+1}^n + (3v^3 - 6v^2 - 3v + 6)C_i^n \\ &+ (-3v^3 + 3v^2 + 6v)C_{i-1}^n + (v^3 - v)C_{i-2}^n]. \end{aligned} \tag{11}$$

Accidentally, the scheme is exactly the QUICKEST scheme.

For the six-node scheme there are three third-order polynomials L_1, L_2 and L_3, passing through C_i^n and C_{i-1}^n. L_k passes through C_{i-k}^n, C_{i-k+1}^n, C_{i-k+2}^n and C_{i-k+3}^n for $k = 1, 2, 3$. The expressions for L_1, L_2 and L_3 are given in Appendix I. To satisfy the four properties, the resulting scheme (6P4O) is given by

$$C_i^{n+1} = (a + b * v) * L_1 + (1 - 2a - b) * L_2 + (a + b - b * v) * L_3, \tag{12}$$

where a and b are free parameters determined as $a = 607/1800$ and $b = -390/1800$. The full expression of the scheme is given by

$$\begin{aligned} C_i^{n+1} = \frac{1}{10800} * [&(390v^4 - 607v^3 - 390v^2 + 607v)C_{i+2}^n \\ &- (1170v^4 + 325v^3 - 7089v^2 + 5594v)C_{i+1}^n \\ &+ (780v^4 + 5570v^3 - 13656v^2 - 3494v + 10800)C_i^n \\ &+ (780v^4 - 8690v^3 + 7734v^2 + 10976v)C_{i-1}^n \\ &- (1170v^4 - 5005v^3 + 906v^2 + 2929v)C_{i-2}^n \\ &+ (390v^4 - 953v^3 + 129v^2 + 434v)C_{i-3}^n]. \end{aligned} \tag{13}$$

For the eight-node scheme there are four fourth-order polynomials K_1, K_2, K_3 and K_4 passing through C_i^n and C_{i-1}^n. The expressions for these polynomials are given in Appendix I. The resulting scheme (8P5O) is given by

$$\begin{aligned} C_i^{n+1} = &(a + b * v) * K_1 + [c + (1 - 2a - b - 2c) * v] * K_2 \\ &+ [(1 - 2a - b - c) - (1 - 2a - b - 2c) * v] * K_3 + [(a + b) - b * v] * K_4, \end{aligned} \tag{14}$$

where a, b and c are free parameters determined as $a = 2465/18000$, $b = -1734/18000$ and $c = 8755/18000$. The full expression of the scheme is given by

$$\begin{aligned} C_i^{n+1} = \frac{1}{432000} * [&(-1734v^5 - 1003v^4 + 6664v^3 + 1003v^2 - 4930v)C_{i+3}^n \\ &+ (4230v^5 + 25115v^4 - 51320v^3 - 25115v^2 + 47090v)C_{i+2}^n \\ &+ (3126v^5 - 82857v^4 + 33952v^3 + 310893v^2 - 265114v)C_{i+1}^n \\ &+ (-18390v^5 + 90665v^4 + 186800v^3 - 582845v^2 - 108230v + 432000)C_i^n \\ &+ (18390v^5 - 1285v^4 - 365560v^3 + 337645v^2 + 442810v)C_{i-1}^n \\ &+ (-3126v^5 - 67227v^4 + 266216v^3 - 53133v^2 - 142730v)C_{i-2}^n \\ &+ (-4230v^5 + 46265v^4 - 91440v^3 + 13915v^2 + 35490v)C_{i-3}^n \\ &+ (1734v^5 - 9673v^4 + 14688v^3 - 2363v^2 - 4386v)C_{i-4}^n]. \end{aligned} \tag{15}$$

Comparing with the corresponding schemes using the highest Lagrangian interpolation polynomials based on Fourier mode analysis, the newly developed schemes are apparently better in terms of phase and amplitude accuracies (Figures 2(a) and 2(b)).

CONSERVATIVE FORM, FLUX LIMITER AND DISCRIMINATOR

The backward characteristics schemes can be rewritten in the conservative form

$$C_i^{n+1} = C_i^n - vC_{i+1/2}^n + vC_{i-1/2}^n. \tag{16}$$

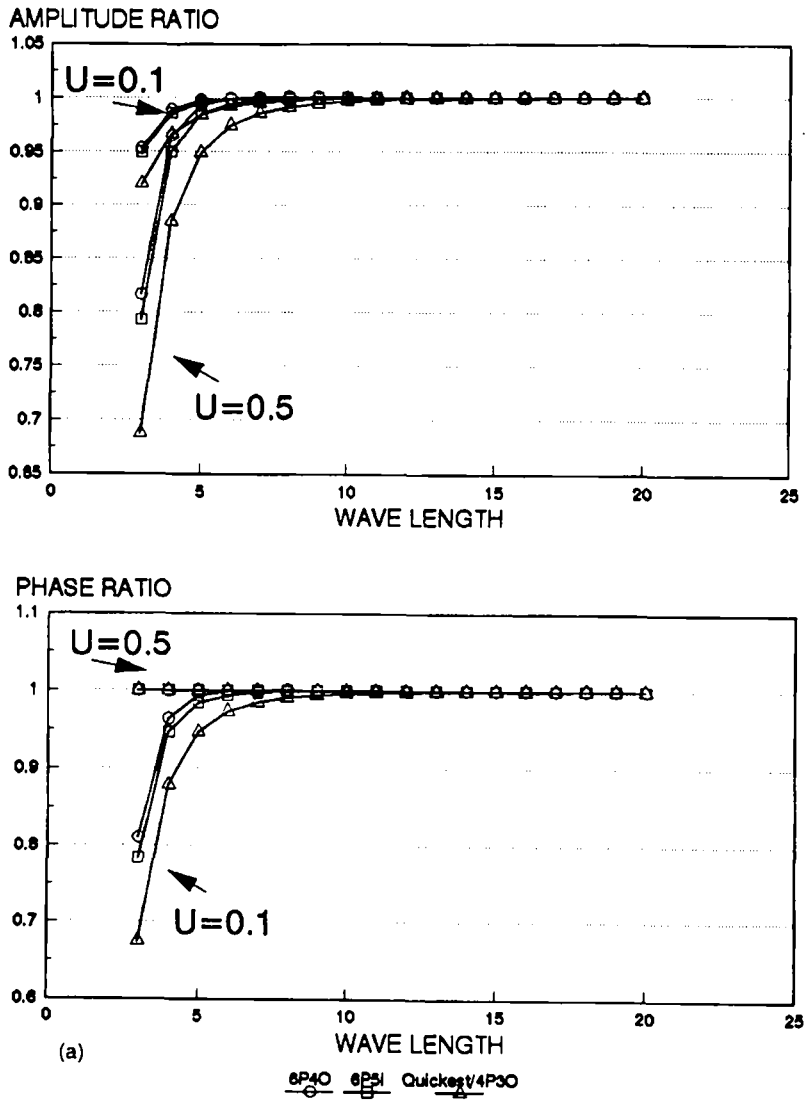

Figure 2. Fourier mode analysis of various schemes: (a) four-point and six-point schemes

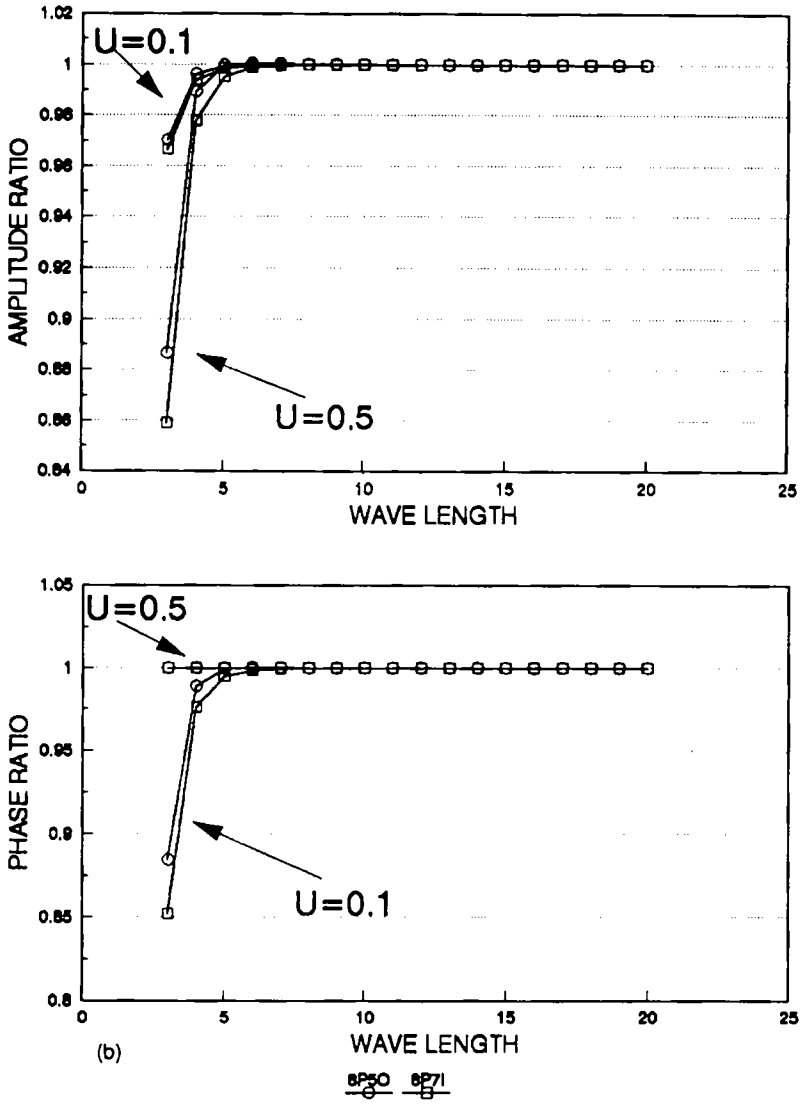

Figure 2. Fourier mode analysis of various schemes: (b) eight-point schemes

For a $2r$-node scheme

$$C^n_{i+1/2} = \sum_{k=-r+1}^{r-1} g_{i+k}(v) C^n_{i+k}, \tag{17}$$

$$C^n_{i-1/2} = \sum_{k=-r}^{r-2} h_{i+k}(v) C^n_{i+k}, \tag{18}$$

where g and h are polynomials in v and $g_{i+k}(v) \equiv h_{i+k-1}(v)$. As an example, for 6P4O it can be

shown that

$$C_{i+1/2}^n = \frac{1}{10800}[(390\nu^3 - 953\nu^2 + 129\nu + 434)C_{i-2}^n - (780\nu^3 - 4052\nu^2 + 777\nu + 2495)C_{i-1}^n$$
$$- (4638\nu^2 - 6957\nu - 8481)C_i^n + (780\nu^3 + 932\nu^2 - 6699\nu + 4987)C_{i+1}^n$$
$$- (390\nu^3 - 607\nu^2 - 390\nu + 607)C_{i+2}^n]. \tag{19}$$

For non-linear advection problems in which the velocity is variable in time and space, the conservative form can be written as

$$C_i^{n+1} = C_i^n - v_{i+1/2}^n C_{i+1/2}^n + v_{i-1/2}^n C_{i-1/2}^n, \tag{20}$$

where

$$C_{i+1/2}^n = \sum_{k=-r+1}^{r-1} g_{i+k}\left(u_{i+1/2}^n \frac{\Delta t}{\Delta x}\right) C_{i+k}^n,$$

$$C_{i-1/2}^n = \sum_{k=-r}^{r-2} h_{i+k}\left(u_{i-1/2}^n \frac{\Delta t}{\Delta x}\right) C_{i+k}^n,$$

$$g_{i+k}(\nu) \equiv h_{i+k-1}(\nu).$$

In situations where sharp fronts exist, non-physical over- and undershoots of the numerical solution appear when the usual finite difference schemes (including backward characteristics schemes) are used. Many flux-limiting schemes have been proposed to eliminate this problem.[12–14]

One advantage of the conservative form of a characteristics-based scheme is that a flux limiter can easily be added to the scheme to prevent the generation of over- and undershoots of the solution, with the conservative property of the scheme being retained. The flux limiter used in the present scheme is due to Leonard and Mokhtari.[14] The underlying assumption used in developing the flux limiter is that the concentration variation is monotonic within the domain bounded by two adjacent nodes. Details of the flux limiter are summarized as follows (ν is assumed constant and positive for easy presentation). (a) If $C_{i-1}^n < C_i^n < C_{i+1}^n$ or vice versa, then first check whether the computed $C_{i+1/2}^n$ lies within the bounded range $[C_i^n, C_{i+1}^n]$; if not, then set $C_{i+1/2}^n$ to its nearest value within the bounded range. Secondly, check whether C_i^{n+1} lies within the bounded range $[C_{i-1}^n, C_i^n]$. This condition can be obtained by tracing the characteristics line passing through node i backwards in time from time level $n+1$ to time level n. By using equation (16) and the inequality $C_{i-1}^n < C_{i-1/2}^n < C_{i+1}^n$ or vice versa, the above condition can be reduced to a more restrictive condition that $C_{i+1/2}^n$ should lie within the bounded range $[C_i^n, C_{i-1}^n + (C_i^n - C_{i-1}^n)/\nu]$. If the computed $C_{i+1/2}^n$ lies outside this range, then set $C_{i+1/2}^n$ to its nearest value within the bounded range. (b) If C_i^n is a local minimum or maximum among the three values C_{i-1}^n, C_i^n and C_{i+1}^n, then set $C_{i+1/2}^n$ equal to C_i^n.

The flux limiter is successful in preventing over- and undershoots of the solution, but it also causes clipping of profiles with sharp curvature. To avoid clipping, the flux limiter should be switched off around the peak of a sharp profile. This requires a mechanism to differentiate between physical peak and numerical oscillations. Leonard and Niknafs[15] have developed a seven-point discriminator to serve this purpose. However, this discriminator will swtich on the flux limiter when the Courant number is 0·5 for some schemes. The reason is that this discriminator does not treat the case where there are two adjacent nodes with the same maximum

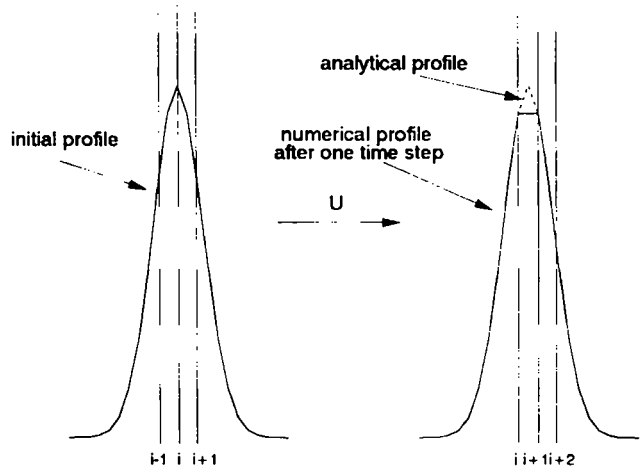

Figure 3. Illustration of the case where the seven-point discriminator fails to work for certain schemes

value as the local maximum (Figure 3). Thus the narrow extreme is clipped by the flux limiter. Moreover, this seven-point discriminator requires considerable computational effort as compared with the numerical scheme itself. To overcome these two shortcomings, a five-point discriminator is developed. The algorithm of the five-point discriminator is given as follows.

Assuming there is a local maximum (a minimum requires the reversal of all the subsequent inequalities described below), the discriminator chooses a stencil of five nodes, C^n_{i-2}, C^n_{i-1}, C^n_i, C^n_{i+1} and C^n_{i+2}, and computes the difference between each pair of consecutive points:

$$D_1 = C^n_{i-1} - C^n_{i-2}, \qquad D_2 = C^n_i - C^n_{i-1}, \qquad D_3 = C^n_{i+1} - C^n_i, \qquad D_4 = C^n_{i+2} - C^n_{i+1}. \quad (21)$$

1. Check whether D_1 and D_2 are positive, D_3 is non-positive and D_4 is negative. If true, then go to step 2; if not, then proceed with the limiter active.
2. Check whether $|D_2| < |D_1|$ and $|D_3| < |D_4|$. If true, switch off the limiter at the current node i and the two adjacent nodes $i - 1$ and $i + 1$; if not, then proceed with the limiter active.

TEST EXAMPLES

The first example is pure advection of a combination of an elliptic profile (half-length of z-axis, 10 cm) and a Gaussian profile (standard deviation 1·5 cm) under constant velocity to compare the performance of the above schemes. The velocity is 0·5 cm s^{-1}. The grid size is 1 cm, the time step is 1 or 0·2 s and the distance travelled is 50 cm. The relative performances of the schemes are in accordance with the Fourier mode analysis (Figures 4 and 5). The present schemes are more accurate than their corresponding schemes using the highest-order Lagrangian polynomial. 2PHC is included in the comparison to represent the class of scheme using a Hermitian polynomial. The performance of this scheme is inferior to that of 6P4O (larger damping of short-wave components; see Figures 4(b) and 5(b).

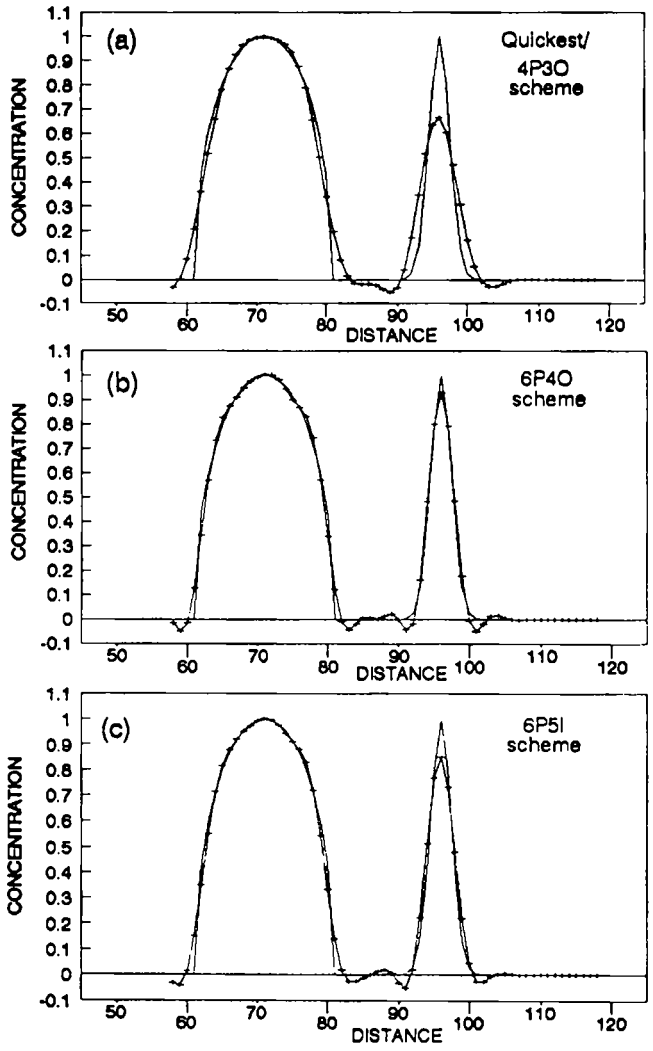

Figure 4. Pure advection of various profiles at Courant number of 0·1: (a) QUICKEST/4P3O; (b) 6P4O; (c) 6P5I

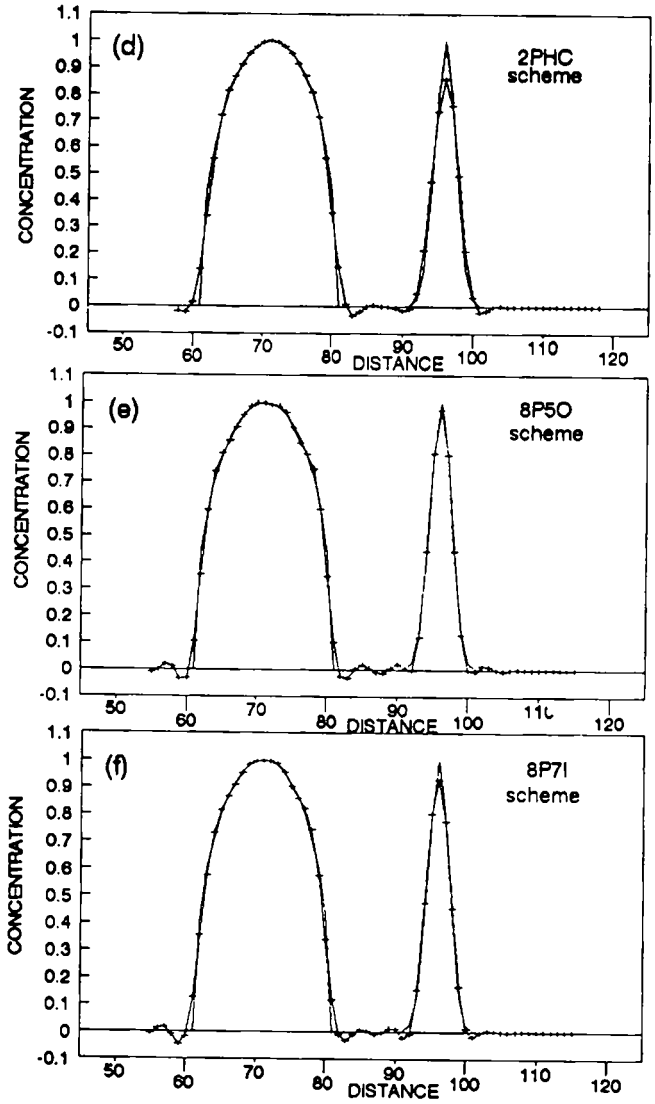

Figure 4. Pure advection of various profiles at Courant number of 0·1: (d) 2PHC; (e) 7P5O; (f) 8P7I

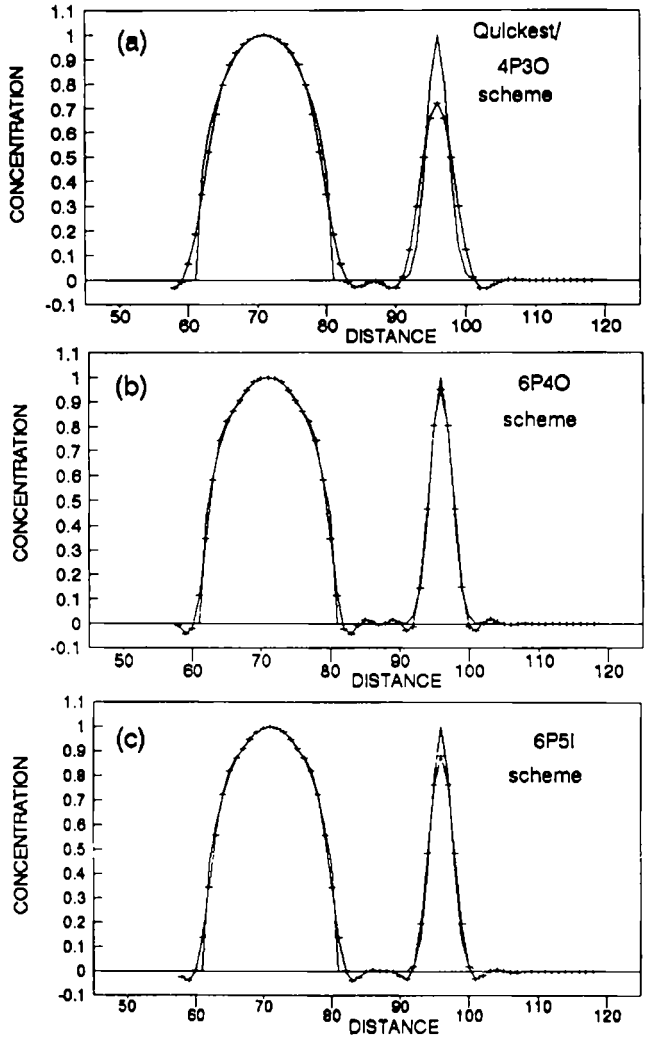

Figure 5. Pure advection of various profiles at Courant number of 0·5: (a) QUICKEST/4P3O; (b) 6P4O; (c) 6P5I

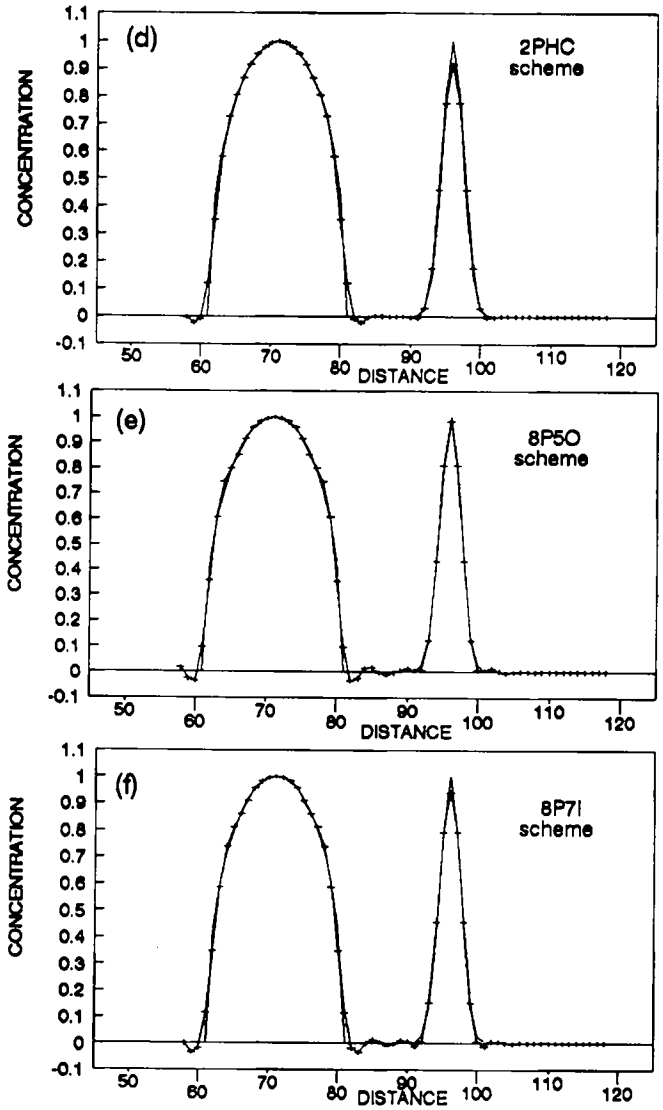

Figure 5. Pure advection of various profiles at Courant number of 0·5: (d) 2PHC; (e) 8P5O; (f) 8P7I

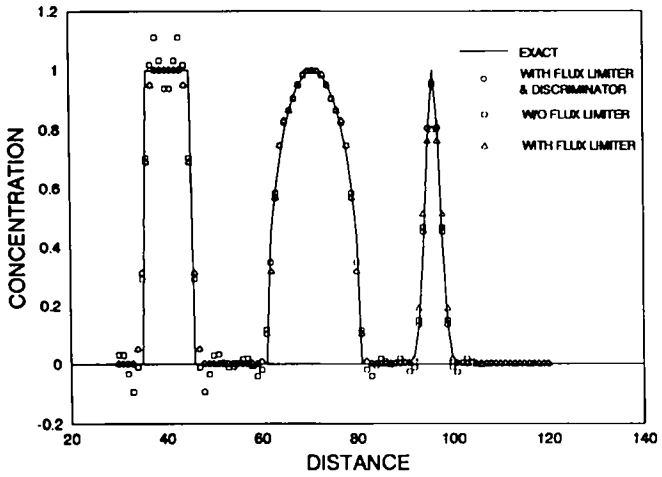

Figure 6. Effect of flux limiter and discriminator

The second example is pure advection of the same profiles plus a square profile (plateau width 9 cm) to illustrate the effect of imposition of the flux limiter and the discriminator. 6P4O is used in the simulation and 90 time steps are run for a Courant number of 0·5. The results are shown in Figure 6. For the square profile, over- and undershoots of the solution are apparent for the original scheme, while the imposition of the flux limiter can prevent this problem. For the Gaussian profile, in contrast, the imposition of the flux limiter causes clipping of the profile, while the switching-off of the flux limiter around the physica peak by the discriminator can eliminate this effect and produce an accurate solution.

The computational times required by the various schemes for the first example are shown in Appendix II. The computational effort required by 6P4O is double that required by 4P3O and about 85% of that required by 6P5I. The computational effort required by 8P5O is 320% of that required by 4P3O and about 80% of that required by 8P7I.

CONCLUSIONS

A subclass of the backward characteristics method in which the interpolative polynomial used is a combination of several lower-order Lagrangian polynomials for a given number of nodes involved in the computation is developed with the aid of Fourier mode analysis. This schemes are efficient, accurate and oscillation-free after the addition of a flux limiter and a modified discriminator.

APPENDIX I: LAGRANGIAN POLYNOMIALS USED IN EQUATIONS (10), (12) and (14)

$$S_1 = \tfrac{1}{2}\nu(1+\nu)C_{i-1}^n + (1-\nu)(1+\nu)C_i^n - \tfrac{1}{2}\nu(1-\nu)C_{i+1}^n,$$

$$S_2 = -\tfrac{1}{2}\nu(1-\nu)C_{i-2}^n + \nu(2-\nu)C_{i-1}^n + \tfrac{1}{2}(1-\nu)(2-\nu)C_i^n,$$

$$L_1 = \tfrac{1}{6}\nu(1+\nu)(2+\nu)C_{i-1}^n + \tfrac{1}{2}(1-\nu)(1+\nu)(2+\nu)C_i^n - \tfrac{1}{2}\nu(1-\nu)(2+\nu)C_{i+1}^n + \tfrac{1}{6}\nu(1-\nu)(1+\nu)C_{i+2}^n,$$

$$L_2 = -\tfrac{1}{6}\nu(1-\nu)(1+\nu)C^n_{i-2} + \tfrac{1}{2}\nu(2-\nu)(1+\nu)C^n_{i-1} + \tfrac{1}{2}(1-\nu)(2-\nu)(1+\nu)C^n_i - \tfrac{1}{6}\nu(1-\nu)(2-\nu)C^n_{i+1},$$

$$L_3 = \tfrac{1}{6}\nu(1-\nu)(2-\nu)C^n_{i-3} - \tfrac{1}{2}\nu(1-\nu)(3-\nu)C^n_{i-2} + \tfrac{1}{2}\nu(2-\nu)(3-\nu)C^n_{i-1} + \tfrac{1}{6}(1-\nu)(2-\nu)(3-\nu)C^n_i,$$

$$K_1 = \tfrac{1}{24}\nu(1+\nu)(2+\nu)(3+\nu)C^n_{i-1} + \tfrac{1}{6}(1-\nu)(1+\nu)(2+\nu)(3+\nu)C^n_i - \tfrac{1}{4}\nu(1-\nu)(2+\nu)(3+\nu)C^n_{i+1} + \tfrac{1}{6}\nu(1-\nu)(1+\nu)(3+\nu)C^n_{i+2} - \tfrac{1}{24}\nu(1-\nu)(1+\nu)(2+\nu)C^n_{i+3},$$

$$K_2 = -\tfrac{1}{24}\nu(1-\nu)(1+\nu)(2+\nu)C^n_{i-2} + \tfrac{1}{6}\nu(2-\nu)(1+\nu)(2+\nu)C^n_{i-1} + \tfrac{1}{4}(1-\nu)(2-\nu)(1+\nu)(2+\nu)C^n_i - \tfrac{1}{6}\nu(1-\nu)(2-\nu)(2+\nu)C^n_{i+1} + \tfrac{1}{24}\nu(1-\nu)(2-\nu)(1+\nu)C^n_{i+2},$$

$$K_3 = \tfrac{1}{24}\nu(1-\nu)(2-\nu)(1+\nu)C^n_{i-3} - \tfrac{1}{6}\nu(1-\nu)(3-\nu)(1+\nu)C^n_{i-2} + \tfrac{1}{4}\nu(2-\nu)(3-\nu)(1+\nu)C^n_{i-1} + \tfrac{1}{6}(1-\nu)(2-\nu)(3-\nu)(1+\nu)C^n_i - \tfrac{1}{24}\nu(1-\nu)(2-\nu)(3-\nu)C^n_{i+1},$$

$$K_4 = -\tfrac{1}{24}\nu(1-\nu)(2-\nu)(3-\nu)C^n_{i-4} + \tfrac{1}{6}\nu(1-\nu)(2-\nu)(4-\nu)C^n_{i-3} - \tfrac{1}{4}\nu(1-\nu)(3-\nu)(4-\nu)C^n_{i-2} + \tfrac{1}{6}\nu(2-\nu)(3-\nu)(4-\nu)C^n_{i-1} + \tfrac{1}{24}(1-\nu)(2-\nu)(3-\nu)(4-\nu)C^n_i.$$

APPENDIX II: COMPUTATIONAL EFFORT REQUIRED BY VARIOUS SCHEMES IN THE FIRST EXAMPLE WITH 200 NODES AND 100 TIME STEPS

Scheme	CPU time (s)
4P3O, QUICKEST	0·22
6P4O	0·44
6P5I	0·52
8P5O	0·71
8P7I	0·88

The computer model used for simulation is a 486 DX-33.

REFERENCES

1. R. Courant, E. Isaacson and M. Rees, 'On the solution of nonlinear hyperbolic differential equations by finite difference', *Commun. Pure Appl. Math.*, V, 243–255 (1952).
2. R. Courant, K. O. Friedrichs and H. Lewy, 'Uber die partiellen differenzengleichurgen der mathematischen physik', *Math. Ann.*, **100**, 32–74 (1928).
3. P. D. Lax and B. Wendroff. 'Systems of conservation laws', *Commun. Pure Appl. Math.*, **13**, 217–237 (1960).
4. J. E. Fromm, 'A method for reducing dispersion in convective difference schemes', *J. Comput. Phys.*, **3**, 176–189 (1968).
5. B. P. Leonard, 'A stable and accurate convective modelling procedure based on quadratic upstream interpolation', *Comput. Methods Appl. Mech. Eng.*, **19**, 59–98 (1979).

6. C. E. Leith, 'Numerical simulation of the Earth's atmosphere', *Methods Comput. Phys.*, **4**, 1–28 (1965).
7. J. P. Benque, G. Labadie and J. Ronat, 'A finite element method for Navier–Stokes equations coupled with a temperature equation', *Proc. 4th Int. Symp. on Finite Elements in Flow Problems*, Tokyo, 1982.
8. B. P. Leonard, 'The ULTIMATE conservative difference scheme applied to unsteady one-dimensional advection', *Comput. Methods Appl. Mech. Eng.*, **88**, 17–74 (1991).
9. C. W. Li, 'Advection simulation by minimax-characteristics method', *J. Hydraul. Eng., ASCE*, **116**, 1138–1144 (1990).
10. F. M. Holly Jr and A. Preissmann, 'Accurate calculation of transport in two dimensions', *J. Hydraul. Div., ASCE*, **103**, 1259–1277 (1977).
11. T. Komatsu, F. M. Holly Jr., N. Nakashiki and K. Ohgushi, 'Numerical calculation of pollutant transport in one and two dimensions', *J. Hydrosci. Hyraul. Eng.*, **3**, (2), 15–30 (1985).
12. J. P. Boris and D. L. Book, 'Flux-corrected transport I. SHASTA, a fluid transport algorithm that works', *J. Comput. Phys.*, **11**, 38–69 (1973).
17. B. van Leer, 'Towards the ultimate conservative difference scheme. V. A second order sequel of Godunov's method', *J. Comput. Phys.*, **32**, 101 (1979).
14. B. P. Leonard and S. Mokhtari, 'Beyond first-order upwinding: the Ultra-sharp alternative for non-oscillatory steady-state simulation of convection', *Int. j. numer. methods in eng.*, **30**, 729–766 (1990).
15. B. P. Leonard and H. S. Niknafs, 'Sharp monotonic resolution of discontinuities without clipping of narrow extrema', *Comput. Fluids*, **19**, 141–154 (1991).